International Journal of Minerals, Metallurgy and Materials
Volume 25, Number 11, November 2018, Page 1275
https://doi.org/10.1007/s12613-018-1680-x

Effect of sintering temperature on the physical properties and electrical contact properties of doped $AgSnO_2$ contact materials

Hai-tao Wang[1,2], *Zi-xiang Wang*[1,2], *Lian-zheng Wang*[1,2], *Jing-qin Wang*[1,2], *and Yan-cai Zhu*[1,2]

1) State Key Laboratory of Reliability and Intelligence of Electrical Equipment, School of Electrical Engineering, Hebei University of Technology, Tianjin 300130, China
2) Key Laboratory of Electromagnetic Field and Electrical Apparatus Reliability of Hebei Province, School of Electrical Engineering, Hebei University of Technology, Tianjin 300130, China
(Received: 13 February 2018; revised: 22 May 2018; accepted: 23 May 2018)

Abstract: $AgSnO_2$ electrical contact materials doped with Bi_2O_3, La_2O_3, and TiO_2 were successfully fabricated by the powder metallurgy method under different initial sintering temperatures. The electrical conductivity, density, hardness, and contact resistance of the $AgSnO_2/Bi_2O_3$, $AgSnO_2/La_2O_3$, and $AgSnO_2/TiO_2$ contact materials were measured and analyzed. The arc-eroded surface morphologies of the doped $AgSnO_2$ contact materials were investigated by scanning electron microscopy (SEM). The effects of the initial sintering temperature on the physical properties and electrical contact properties of the doped $AgSnO_2$ contact materials were discussed. The results indicate that the physical properties can be improved and the contact resistance of the $AgSnO_2$ contact materials can be substantially reduced when the materials are sintered under their optimal initial sintering temperatures.

Keywords: sintering temperature; contact materials; physical properties; electrical contact properties

1. Introduction

Electrical contact materials are core components of contactors, relays, circuit breakers, switchgears, and other electrical equipment. The main function of electrical contact materials is connecting and disconnecting a circuit. To ensure high reliability of electrical equipment, electrical contact materials with high performance are also important [1].

$AgSnO_2$, which is a contact material with excellent anti-welding properties and resistance to arc erosion, has been used in low-voltage electrical equipment [2]. Although $AgSnO_2$ has shown good prospects as a contact material because it is environmentally benign and demonstrates remarkable performance, it also presents some drawbacks, such as unstable contact resistance and poor ductility and malleability [3]. Two approaches to improving the properties of $AgSnO_2$ contact materials have been reported. One approach is to choose a suitable additive to modify the electrical contact material itself [4–7]; the other approach is to improve the electrical properties through modification of the preparation method [8–9].

The methods used to prepare $AgSnO_2$ contact materials include the powder metallurgy method, the internal oxidation method, etc. [10–13]. The powder metallurgy method is widely used in the preparation of $AgSnO_2$ contact materials. Sintering is a critical step in the powder metallurgy method and strongly influences the properties of electrical contact materials [14–17]. Therefore, elucidating the optimal sintering temperature and improving the properties of the electrical contact material are worthwhile topics of investigation.

In the present work, $AgSnO_2$ contact materials with different additives were fabricated by the powder metallurgy method under different initial sintering temperatures. The influence of the initial sintering temperature on the physical properties and electrical contact properties of doped $AgSnO_2$ contact materials were explored. Meanwhile, the microstructure of doped $AgSnO_2$ contact materials after arc erosion were investigated.

2. Experimental

2.1. Selection of composition and ratio

The wettability of $AgSnO_2$ contact materials with differ-

Corresponding author: Zi-xiang Wang E-mail: aaron_bjtu@163.com
© University of Science and Technology Beijing and Springer-Verlag GmbH Germany, part of Springer Nature 2018
Springer

ent contents of three additives is shown in Fig. 1. As shown in Fig. 1, when the nominal contents of Bi_2O_3, La_2O_3, and TiO_2 are 1.5wt%, 2.5wt%, and 1.0wt%, respectively, the wetting angle is the minimum, exhibiting the best wettability [18]. Better wettability implies a smaller contact resistance of the materials. The additive proportions based on the analysis results are shown in Table 1.

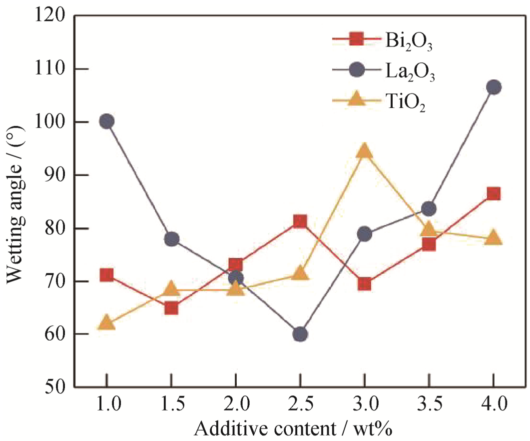

Fig. 1. Wetting angles of doped $AgSnO_2$ contact materials.

Table 1. Compositions and ratios of the investigated contact materials

Composition	Mass ratio
Ag: SnO_2: Bi_2O_3	88.0:10.5:1.5
Ag: SnO_2: La_2O_3	88.0:9.5:2.5
Ag: SnO_2: TiO_2	88.0:11.0:1.0

The purity of the Ag power was 99.95%, and its grain size was 200 mesh. The purity of the SnO_2 power was 99.5%, and its grain size was 800 nm. The purity of the Bi_2O_3, La_2O_3, and TiO_2 powders was 99.9%, and their grain size was 200 nm.

2.2. Preparation of samples

The process of preparation by the powder metallurgy method is shown in Fig. 2. The drying temperature was set as 120°C, and the drying time was 60 min. The ball-mill time was set as 120 min, and the speed was 500 r/min under the positive and negative orientation. The powders were dry-ground, and the ball-to-powder mass ratio was 50% [19]. The balls used to mix the powder included large balls (diameter: 10 mm), medium balls (8 mm), and small balls (6 mm). The grain size of the ball-milled powder ranged between 1 and 30 μm, and its bulk density was 3.287 g/cm^3 (standard deviation: 0.26). The ball-milled powders were formed into cylindrical samples using a 769YP-24B pressed powder machine. The diameter and thickness of the initial pressed samples were 20 mm and 4 mm, respectively. The initial pressure was confirmed at 38 MPa with a dwell time of 5 min. After the initial press, the powers were sintered by an energy-saving box-type electric furnace under vacuum. The heating rate was set as 10°C/min. The composite powders were repressed on a TYE-1000B pressure testing apparatus. The repress was confirmed at 58 MPa with a dwell time of 5 min. The pressed samples were cut into simple cylindrical contacts whose diameter and thickness were 4.5 mm and 4 mm, respectively.

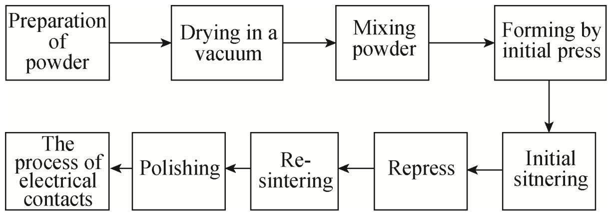

Fig. 2. Preparation process of electrical contact materials.

2.3. Sintering process

The initial sintering process was divided into three stages. The sintering temperature was 240°C for the pre-sintering stage at low temperature and 480°C for the middle stage. The initial sintering temperature in this study refers to the sintering temperature at the third stage. The initial sintering temperature was in the range of 0.6 to 0.95 of the melting point of Ag (961.78°C). Thus, the initial sintering temperature was selected in increments of 60°C in the range from 576 to 912°C. The temperature program used in the sintering process is shown in Fig. 3.

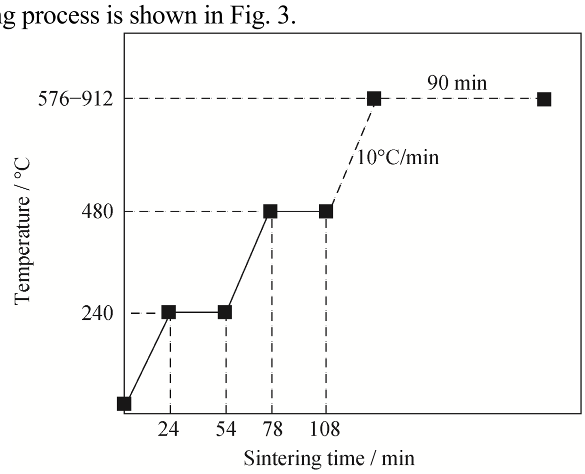

Fig. 3. Initial sintering process.

The $AgSnO_2/Bi_2O_3$ contact material was sintered at an initial sintering temperature of 640, 700, 760, 820, 880, or 920°C and a re-sintering temperature of 820°C. The $AgSnO_2/TiO_2$ contact material was sintered at an initial sintering temperature of 580, 640, 700, 760, 820, or 880°C and a re-sintering temperature of 640°C. Because of the special property of La_2O_3, the $AgSnO_2/La_2O_3$ contact material exhibited low physical properties when sintered at 820°C and 640°C. Therefore, the initial sintering temperature was selected in 30°C increments in the range from 700 to 820°C. Thus, the $AgSnO_2/La_2O_3$ contact material was sintered with an initial sintering temperature of 700, 730, 760, 790, or 820°C and a re-sintering temperature of 760°C.

2.4. Experimental procedure

The conductivity, density, and hardness of the doped $AgSnO_2$ contact materials were measured after the samples were re-sintered. The density was measured at room temperature on the basis of the Archimedes drainage method, and the values were the average of three measurement results. The liquid medium was distilled water. The hardness was measured with a HXD-1000TM microscope tester, and the values were the average of three measurement results. The indentation load was 500 N, and the time under maximum load was 5 s. The conductivity was measured with a SIGMASCOPE SMP10. To ensure the accuracy of the measurements, three measurement points were selected at different positions on the surface of each sample. Each point was measured four times, and the final reported values are the average of the four results.

The electrical contact performance of the doped $AgSnO_2$ contact material at different sintering temperatures was tested by a JF04C electrical contact material test system. The contact mode was surface contact. The measurement voltage was direct current (DC) 24 V. The measurement current was DC 13 A. The contact pressure was 86 cN. The contact pitch was 2.0 mm. The test load was resistive. The contact breaking cycle was 800 ms. Each test sample was made into a pair of cylindrical contacts. The number of make-and-break operations was 25000 per contact. The contact resistance was measured after each 100 normal make-and-break operations. The surface morphologies of the doped $AgSnO_2$ electrical contacts after arc erosion were investigated by scanning electron microscopy (SEM; Nova NanoSEM 450).

3. Results and discussion

3.1. Physical properties of doped $AgSnO_2$ contact materials

The conductivity, density, and hardness data for the $AgSnO_2/Bi_2O_3$, $AgSnO_2/La_2O_3$, and $AgSnO_2/TiO_2$ contact materials at different initial sintering temperatures are shown in Figs. 4–6, respectively.

The results in Figs. 4–6 show that the trends of conductivity, density, and hardness of the doped $AgSnO_2$ contact materials change depending on the additive and the initial sintering temperature. According to the experiment data in

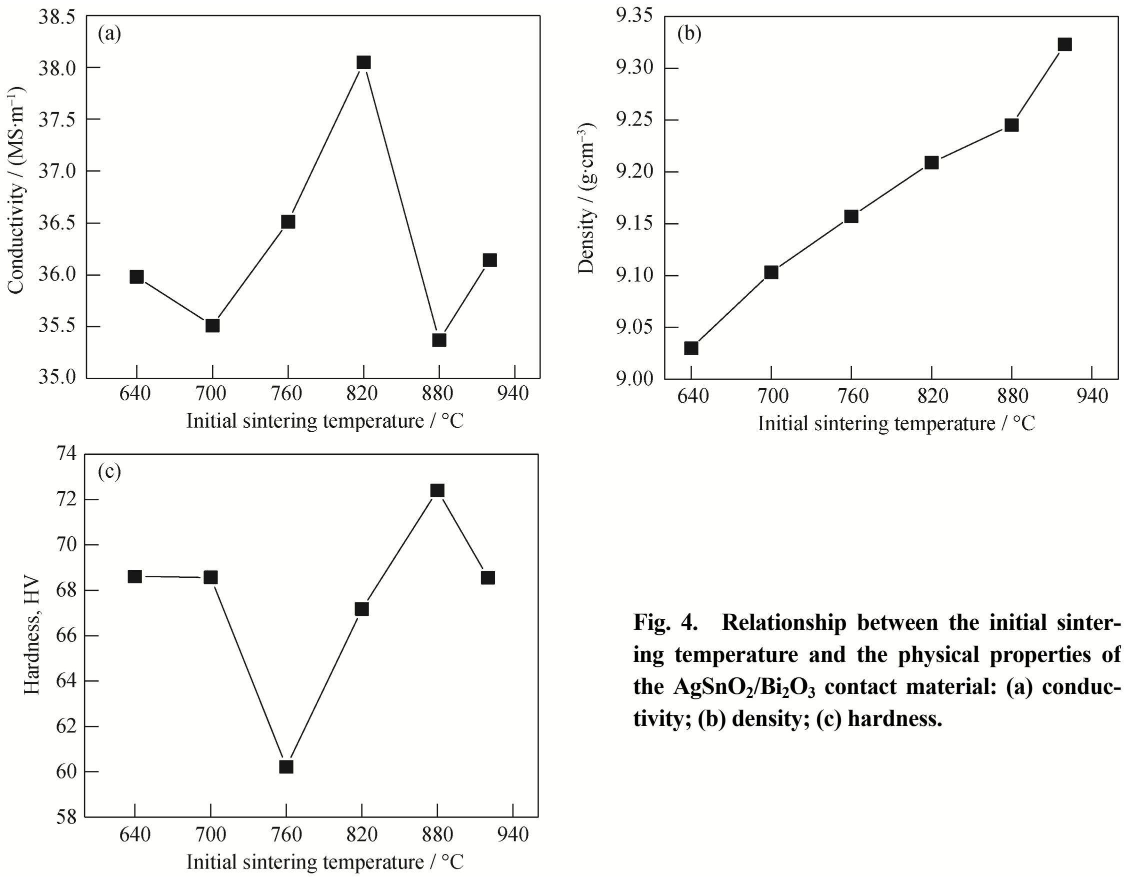

Fig. 4. Relationship between the initial sintering temperature and the physical properties of the $AgSnO_2/Bi_2O_3$ contact material: (a) conductivity; (b) density; (c) hardness.

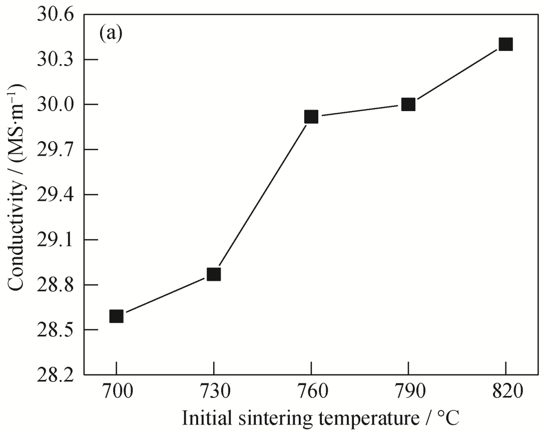

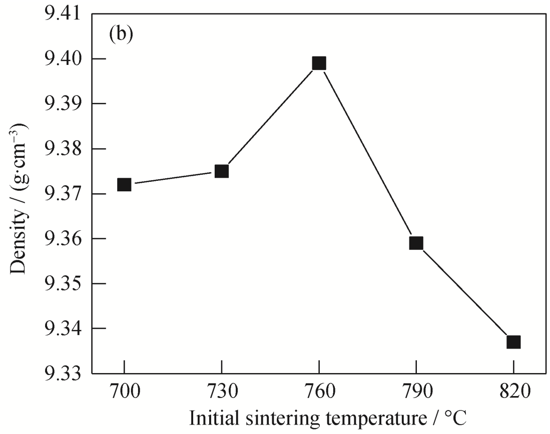

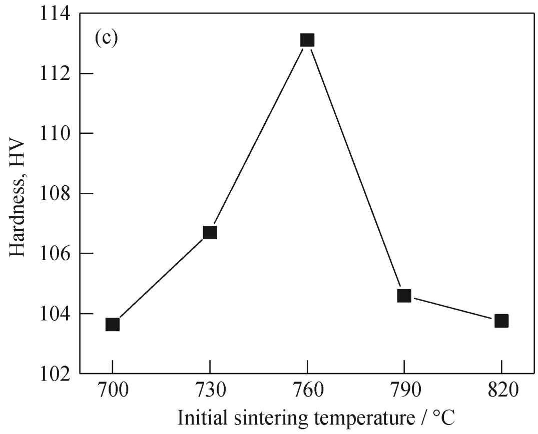

Fig. 5. Relationship between the initial sintering temperature and the physical properties of the $AgSnO_2/La_2O_3$ contact material: (a) conductivity; (b) density; (c) hardness.

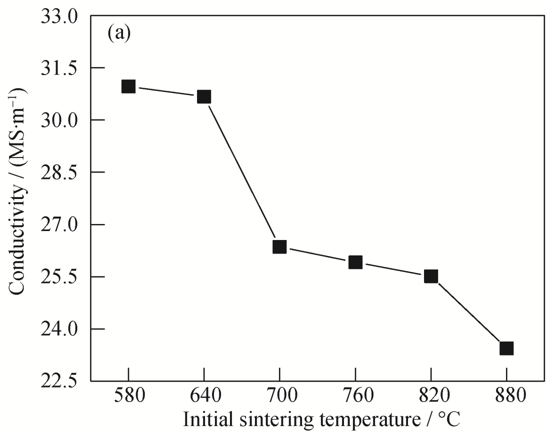

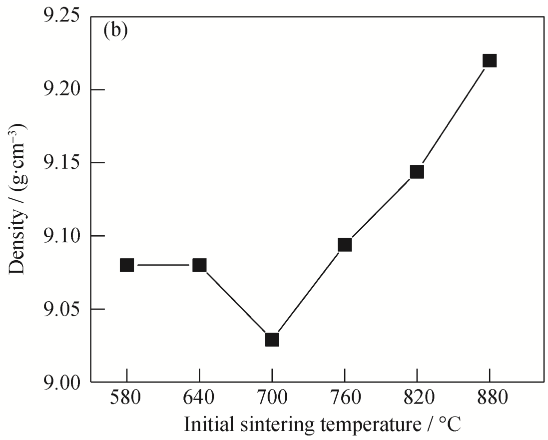

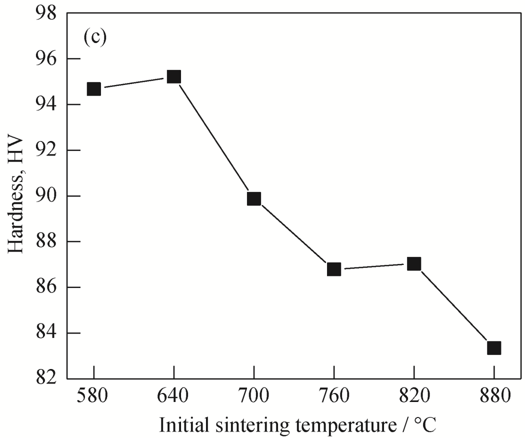

Fig. 6. Relationship between the initial sintering temperature and the physical properties of the $AgSnO_2/TiO_2$ contact material: (a) conductivity; (b) density; (c) hardness.

Figs. 4–6, the conductivity is relatively larger and the density and hardness are in the appropriate range when doped $AgSnO_2$ contact materials are sintered at the optimal initial sintering temperature: 820°C for $AgSnO_2/Bi_2O_3$, 760°C for $AgSnO_2/La_2O_3$, and 640°C for $AgSnO_2/TiO_2$.

The kinetic energy of atoms and their diffusion rate increase with increasing initial sintering temperature. Therefore, in general, a higher sintering temperature results in a greater shrinkage amplitude and in greater conductivity, density, and hardness for samples sintered for the same duration expect for the $AgSnO_2/TiO_2$ contact material. When the initial sintering temperature is too high, the pores shrink too fast because of the rapid atomic diffusion rate; thus, the closed pores leave a large amount of gas. As a result, the volume of the sintered body expands, causing the density and hardness to decrease. For the $AgSnO_2/TiO_2$ contact material with a high initial sintering temperature, the allotropic transformation of TiO_2 from the anatase phase to the rutile phase will change the grains and expand the volume, resulting in the anti-densification phenomenon. Thus, the conductivity and density of the $AgSnO_2/TiO_2$ contact material decrease with an increase in initial sintering temperature, as shown in Figs. 6(a) and 6(c).

3.2. Electrical contact properties of doped $AgSnO_2$ contact materials

The contact resistance data for the $AgSnO_2/Bi_2O_3$, $AgSnO_2/La_2O_3$, and $AgSnO_2/TiO_2$ contact materials sintered at different initial sintering temperatures are shown in Figs. 7–9.

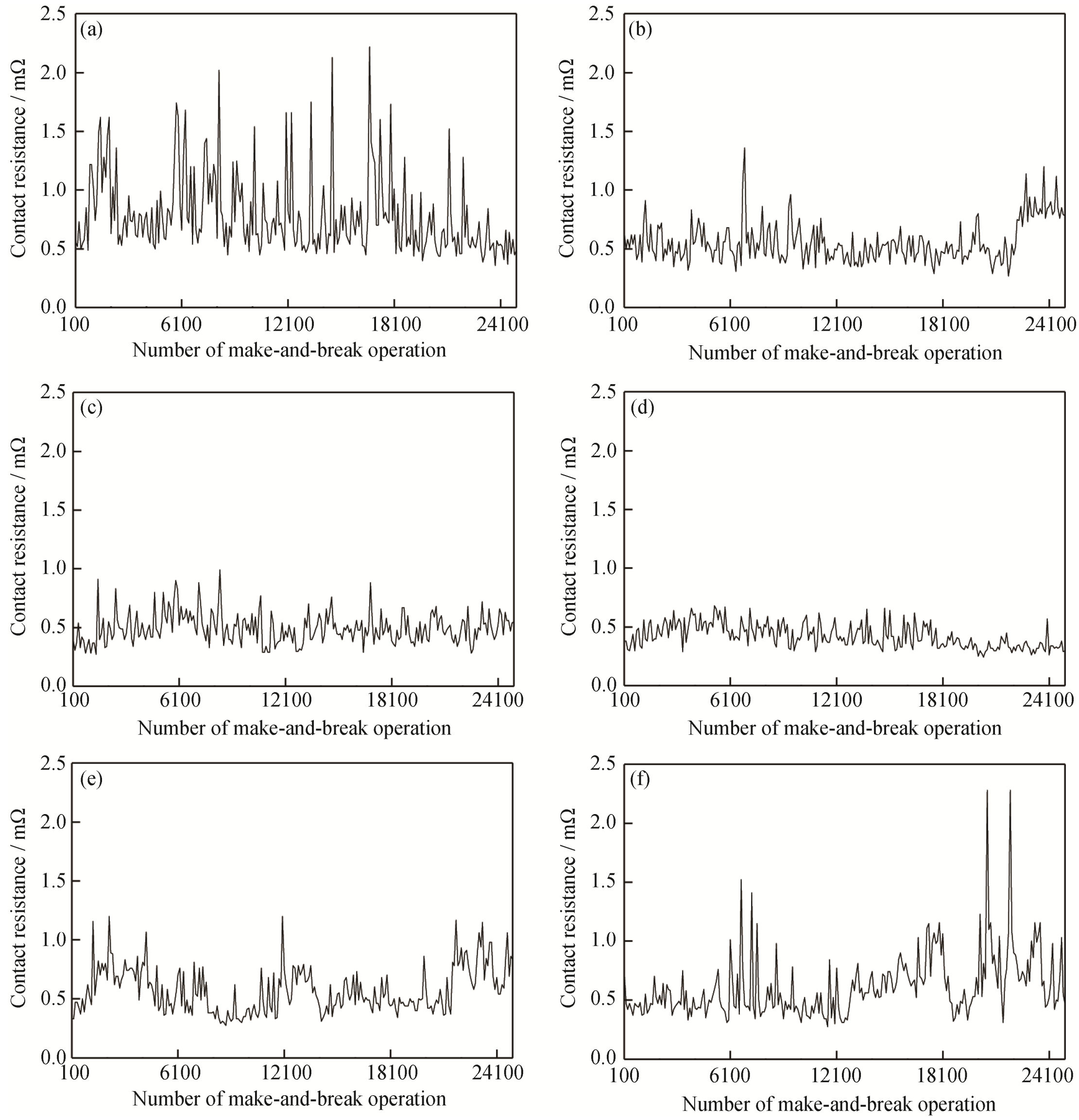

Fig. 7. Contact resistance of the $AgSnO_2/Bi_2O_3$ contact material sintered at different initial sintering temperatures: (a) 640°C; (b) 700°C; (c) 760°C; (d) 820°C; (e) 880°C; (f) 920°C.

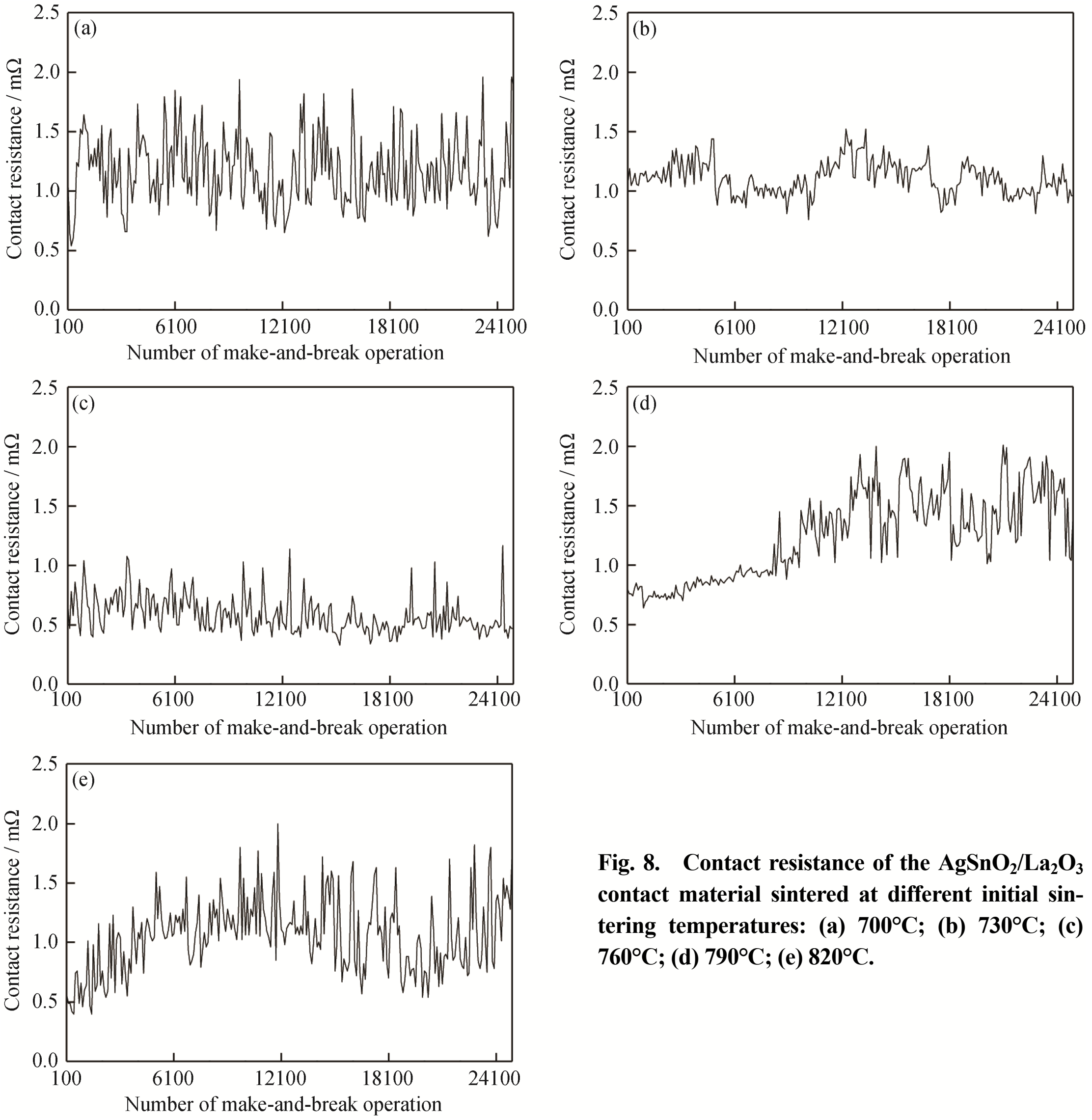

Fig. 8. Contact resistance of the $AgSnO_2/La_2O_3$ contact material sintered at different initial sintering temperatures: (a) 700°C; (b) 730°C; (c) 760°C; (d) 790°C; (e) 820°C.

The specific range and the average value of the contact resistance of the $AgSnO_2/Bi_2O_3$, $AgSnO_2/La_2O_3$, and $AgSnO_2/TiO_2$ contact materials sintered at different initial sintering temperatures are shown in Tables 2–4.

Fig. 7 shows that the contact resistance of the $AgSnO_2/Bi_2O_3$ contact material sintered at 820°C exhibits less fluctuation than that sintered at other initial sintering temperatures. The contact resistance of $AgSnO_2/La_2O_3$ contact material sintered at 760°C has relatively less fluctuation than that sintered at other initial sintering temperatures, as shown in Fig. 8. As evident from Fig. 9, the contact resistance of the $AgSnO_2/TiO_2$ contact material sintered at 640°C exhibits relatively less fluctuation than that sintered at other initial sintering temperatures.

The minimum average contact resistance for the doped $AgSnO_2$ contact materials was obtained under different initial sintering temperatures according to the experiment data in Tables 2, 3, and 4. The minimum average contact resistance of the $AgSnO_2/Bi_2O_3$ contact material was 0.42 mΩ when the initial sintering temperature was 820°C. The minimum average contact resistance of the $AgSnO_2/La_2O_3$ contact material was 0.58 mΩ when the initial sintering temperature was 760°C. The minimum average contact resistance of the $AgSnO_2/TiO_2$ contact material was 0.54 mΩ when the initial sintering temperature was 640°C.

When the initial sintering temperature is too low or too high, the performance of the $AgSnO_2/Bi_2O_3$, $AgSnO_2/La_2O_3$, and $AgSnO_2/TiO_2$ contact materials is poor and the contact resistance is large and unstable. Specifically, when the initial sintering temperature is too low, the activity of particles in the material is low and the atom mobility is poor. As a result, the contact material is not fully sintered and the contact resistance is large and unstable. When the sintering temperature is too high, the activity of the particles is too high, causing the sintered body to expand violently. Especially for the $AgSnO_2/TiO_2$ contact material, the allotropic transformation of TiO_2 from the anatase phase to the rutile phase will result in a change in the grains and an expansion of the volume. The anti-densification phenomenon occurs; consequently, the contact resistance becomes large and unstable.

3.3. SEM analysis

The surface morphologies of the $AgSnO_2/Bi_2O_3$, $AgSnO_2/La_2O_3$, and $AgSnO_2/TiO_2$ contact materials sintered at different initial sintering temperatures and after arc erosion were observed by SEM, and the results are shown in shown Figs. 10–12, respectively.

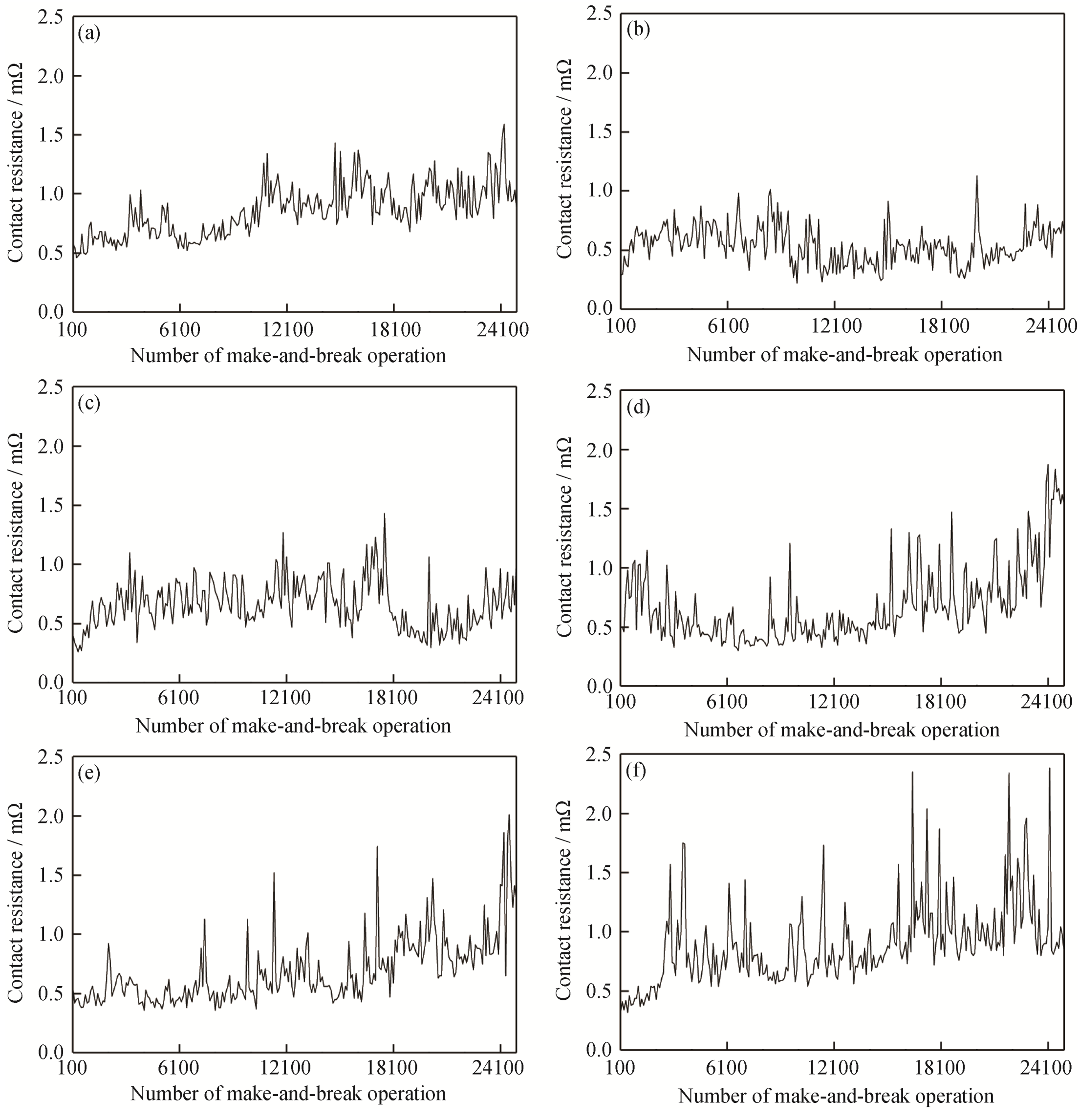

Fig. 9. The contact resistance of the $AgSnO_2/TiO_2$ contact material sintered at different initial sintering temperatures: (a) 580°C; (b) 640°C; (c) 700°C; (d) 760°C; (e) 820°C; (f) 880°C.

Table 2. Contact resistance of the $AgSnO_2/Bi_2O_3$ contact material sintered at different initial sintering temperatures

Initial sintering temperature / °C	Range of contact resistance / mΩ	Average contact resistance / mΩ	Standard deviation / 10^{-2}
640	0.36–2.22	0.78	34.2
700	0.27–1.36	0.56	17.2
760	0.27–0.99	0.49	12.9
820	0.24–0.68	0.42	10.2
880	0.27–1.20	0.57	19.4
920	0.27–2.28	0.61	27.1

Table 3. Contact resistance of the $AgSnO_2/La_2O_3$ contact material sintered at different initial sintering temperatures

Initial sintering temperature / °C	Range of contact resistance / mΩ	Average contact resistance / mΩ	Standard deviation / 10^{-2}
700	0.54–1.96	1.17	29.8
730	0.76–1.52	1.11	13.9
760	0.33–1.17	0.58	15.7
790	0.64–2.01	1.25	36.3
820	0.40–2.00	1.05	31.7

Table 4. The contact resistance of the $AgSnO_2/TiO_2$ contact material sintered at different initial sintering temperatures

Initial sintering temperature / °C	Range of contact resistance / mΩ	Average contact resistance / mΩ	Standard deviation / 10^{-2}
580	0.46–1.59	0.86	21.7
640	0.22–1.13	0.54	16.1
700	0.26–1.43	0.66	20.3
760	0.30–1.87	0.67	31.9
820	0.36–2.01	0.69	28.3
880	0.32–2.38	0.89	34.3

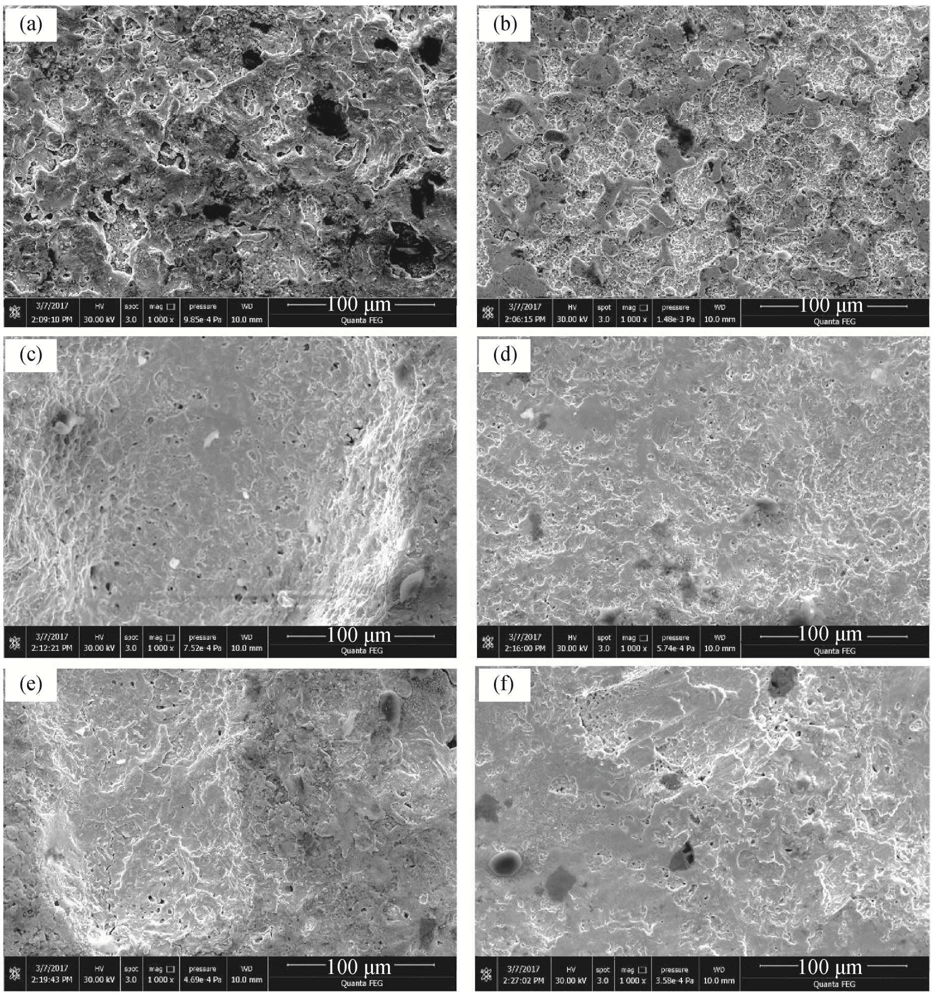

Fig. 10. Surface morphologies of the $AgSnO_2/Bi_2O_3$ contact material sintered at different initial sintering temperatures: (a) 640°C; (b) 700°C; (c) 760°C; (d) 820°C; (e) 880°C; (f) 920°C.

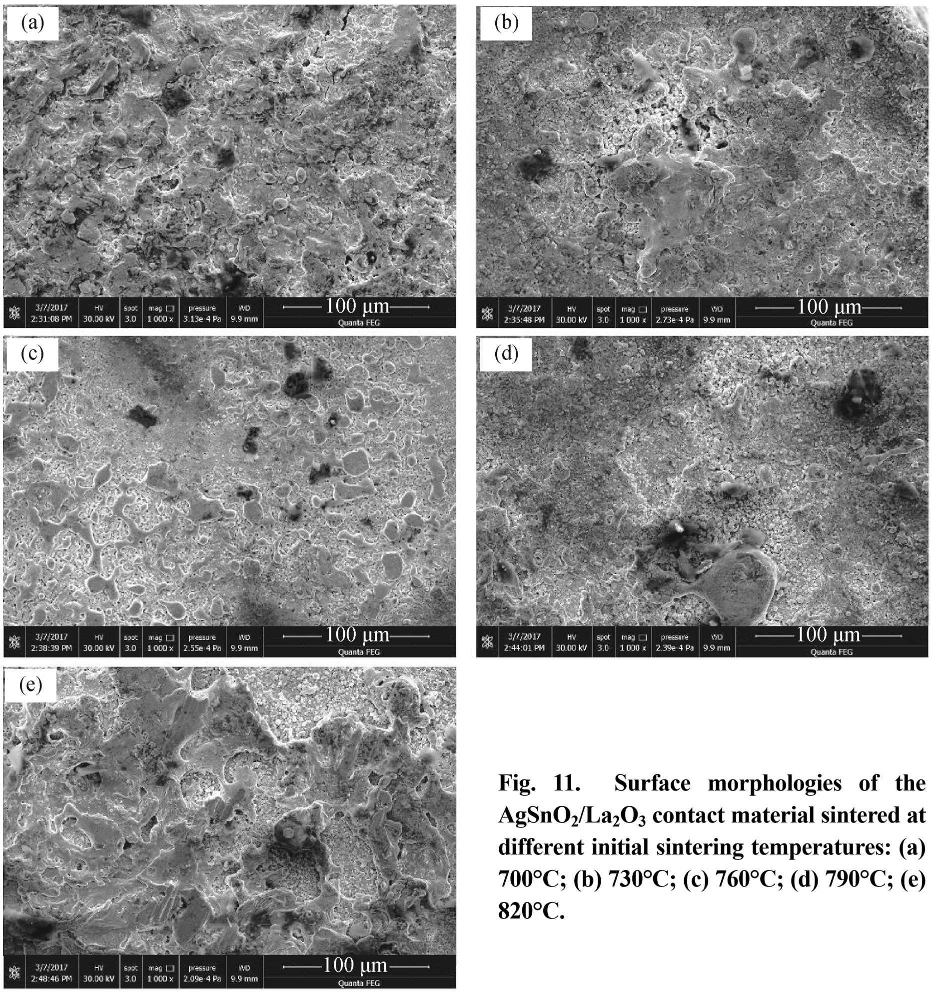

Fig. 11. Surface morphologies of the $AgSnO_2/La_2O_3$ contact material sintered at different initial sintering temperatures: (a) 700°C; (b) 730°C; (c) 760°C; (d) 790°C; (e) 820°C.

Figs. 10(a)–10(b) shows that arc erosion occurs on a larger area of the $AgSnO_2/Bi_2O_3$ contact material sintered at 640°C and 700°C; this arc erosion area is the same as that of the $AgSnO_2/TiO_2$ contact material sintered at 760°C, as shown in Fig. 12(d).

Figs. 10–12 show that the surface morphologies of the doped $AgSnO_2$ electrical contact material is relatively flat, free of holes, and very dense when sintered under the optimum sintering temperature: 820°C for $AgSnO_2/Bi_2O_3$, 760°C for $AgSnO_2/La_2O_3$, and 640°C for $AgSnO_2/TiO_2$. Some SnO_2 particles are observed to distribute uniformly in the melt-spinning microstructure, as shown in Figs. 10(d), 11(c), and 12(b), indicating that the optimal sintering temperature promotes the engulfing of the SnO_2 particles in the Ag melt.

4. Conclusions

Doped $AgSnO_2$ contact materials were prepared by the powder metallurgy method at different initial sintering temperatures. The effects of the initial sintering temperature on the physical properties and electrical contact properties of the doped $AgSnO_2$ contact materials were investigated through measurements and analysis of their conductivity, density, hardness, and contact resistance.

(1) The doped $AgSnO_2$ contact materials exhibit better performance when sintered at the appropriate initial sintering temperature, and the optimal initial sintering temperature of $AgSnO_2$ contact materials differs depending on the additive.

(2) The optimal initial sintering temperatures of the $AgSnO_2/Bi_2O_3$, $AgSnO_2/La_2O_3$, and $AgSnO_2/TiO_2$ contact materials are 820°C, 760°C, and 640°C, respectively.

(3) The $AgSnO_2$ contact material doped with Bi_2O_3 is the most suitable for replacing AgCdO contact materials in low-voltage switching devices.

Acknowledgements

This work is financially supported by the National Natural Science Foundation of China (No. 51777057), the Natural Science Foundation of Hebei Province, China (No. E2016202106), and the Science and Technology Research Project of Colleges and Universities in Hebei Province, China (No. ZD2016078).

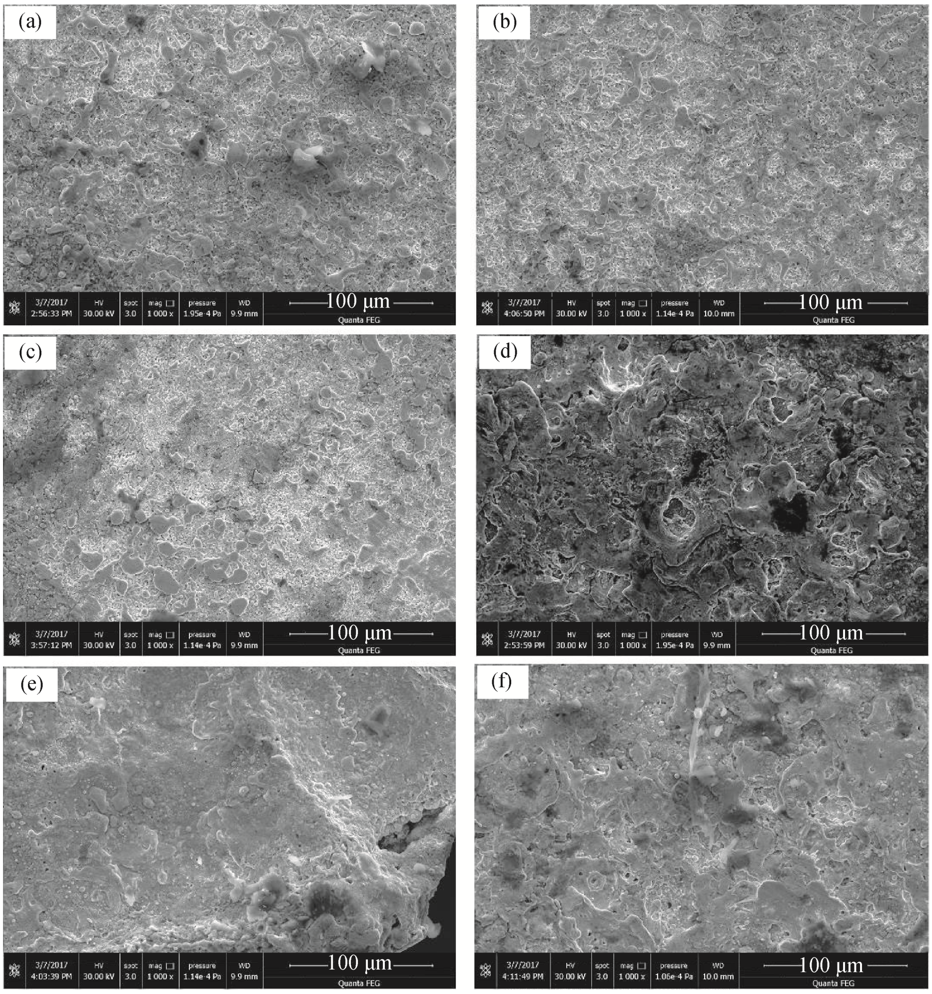

Fig. 12. Surface morphologies of the $AgSnO_2/TiO_2$ contact material sintered at different initial sintering temperatures: (a) 580°C; (b) 640°C; (c) 700°C; (d) 760°C; (e) 820°C; (f) 880°C.

References

[1] D. Jeannot, J. Pinard, P. Ramoni, and E.M. Jost, Physical and chemical properties of metal oxide additions to $AgSnO_2$ contact materials and predictions of electrical performance, *IEEE Trans. Compon. Packag. Manuf. Technol. Part A*, 17(1994), No. 1, p. 17.

[2] O. Nilsson, F. Hauner, and D. Jeannot, Replacement of AgCdO by $AgSnO_2$ in DC contactors, [in] *Proceedings of the 50th IEEE Holm Conference on Electrical Contacts and the 22nd International Conference on Electrical Contacts Electrical Contacts,* Seattle, 2004, p. 70.

[3] F. Hauner, D. Jeannot, K. McNeilly, and J. Pinard, Advanced $AgSnO_2$ contact materials for the replacement of AgCdO in high current contactors, [in] *Electrical Contacts - 2000. Proceedings of the Forty-Sixth IEEE Holm Conference on Electrical Contacts* (*Cat. No. 00CB37081*), Chicago, 2000, p. 225.

[4] Y. Zhu and J. Wang, Preparation and study on performance for silver rare-earth alloy electrical contact materials, [in] *2010 Proceedings of the 56th IEEE Holm Conference on Electrical Contacts*, Charleston, 2010, p. 1.

[5] H. Zoz, H. Ren, and N. Späth, Improved Ag–SnO_2 electrical contact material produced by mechanical alloying, *Metall*, 53(1999), No. 7-8, p. 423.

[6] F. Findik and H. Uzun, Microstructure, hardness and electrical properties of silver-based refractory contact materials, *Mater. Des.*, 24(2003), No. 7, p. 489.

[7] Z.J. Lin, S.H. Liu, J.G. Li, J.L. Chen, M. Xie, X.D. Li, M. Zhang,Q. Zhu, D. Huo, and X.D. Sun , Morphology-controllable synthesis and thermal decomposition of Ag and Ni oxalate for Ag-Ni alloy electrical contact materials, *Mater. Des.*, 108(2016), p. 640.

[8] T.Z. Yang, Z.J. Du, Y.Y. Gu, X.Y. Qiu, and M.X. Jiang, Preparation of $AgSnO_2$ composite powders by hydrothermal process, *J. Cent. South Univ. Technol.*, 14(2007), No. 2, p.

176.

[9] L. Chi, E. Streicher, and D. Fitzgerald, Welding behavior of $AgSnO_2$ contact material with microstructure and additive modifications, [in] *Electrical Contacts, 2004. Proceedings of the 50th IEEE Holm Conference on Electrical Contacts and the 22nd International Conference on Electrical Contacts*, Seattle, 2004, p. 64.

[10] C. Leung, E. Streicher, D. Fitzgerald, and J. Cook, Contact erosion of $AgSnO_2/In_2O_3$ made by internal oxidation and powder metallurgy, [in] *Proceedings of the Fifty-First IEEE Holm Conference on Electrical Contacts,* Chicago, 2005, p. 22.

[11] L.Q. Liu, X.F. Yan, W. Weng, J.F. Xie, and N. Zheng, The investigation on the production process of $AgSnO_2$ Contact Materials by AgSn alloy powder pre-oxidation, [in] *26th International Conference on Electrical Contacts* (*ICEC 2012*), Beijing, 2012, p. 362.

[12] V. Ćosović, N. Talijan, D. Živković, D. Minić, and Ž. Živković, Comparison of properties of silver–metal oxide electrical contact materials, *J. Min. Metall. Sect. B*, 48(2012), No. 1, p. 131.

[13] X.Q. Qiao, Q.H. Shen, L.J. Zhang, L. Chen, X.P. Fan, and H. Yang, A novel method for the preparation of Ag/SnO_2 electrical contact materials, *Rare Met. Mater. Eng.*, 43(2014), No. 11, p. 2614.

[14] X.M. Liu, S.L. Wu, P.K. Chu, C.Y. Chung, J. Zheng, and S.L. Li, Effects of coating process on the characteristics of $Ag–SnO_2$ contact materials, *Mater. Chem. Phys.*, 98(2006), p. 477.

[15] E. Brisson, P. Carre, H. Desplats, P. Rogeon, V. Keryvin, and A. Bonhomme, Effective thermal and electrical conductivities of $AgSnO_2$ during sintering. Part I: Experimental characterization and mechanisms, *Metall. Mater. Trans. A*, 47(2016), No. 12, p. 6304.

[16] I. Smiljanić, A. Smontara, A. Bilušić, N. Barišić, D. Stanić, J. Lukatela, J. Dolinšek, M. Feuerbacher, and B. Grushko., Thermal and electrical conductivities in Al-based complex metallic alloys, *Philos. Mag.*, 88(2008), No. 13-15, p. 2155.

[17] S. Aksöz and N. Maraşl, Thermal and electrical conductivities of silver–indium–tin alloys, *J. Phys. Chem. Solids*, 73(2012), No. 7, p. 902.

[18] Y. Liu, *Effect of Wettability on the Electrical Contact Properties of $AgSnO_2$ Contact Materials* [Dissertation], Hebei University of Technology, Tianjin, 2015, p. 22.

[19] N. Setoudeh, M.H. Paydar, and M. Sajjadnejad, Effect of high energy ball milling on the reduction of nickel oxide by zinc powder, *J. Alloys Compd.*, 623(2015), p. 117.